

Composition and Structure of the Martian Upper Atmosphere: Analysis of Results from Viking



M. B. McElroy; T. Y. Kong; Y. L. Yung; A. O. Nier

Science, New Series, Volume 194, Issue 4271 (Dec. 17, 1976), 1295-1298.

Stable URL:

<http://links.jstor.org/sici?sici=0036-8075%2819761217%293%3A194%3A4271%3C1295%3ACASOTM%3E2.0.CO%3B2-B>

Your use of the JSTOR archive indicates your acceptance of JSTOR's Terms and Conditions of Use, available at <http://www.jstor.org/about/terms.html>. JSTOR's Terms and Conditions of Use provides, in part, that unless you have obtained prior permission, you may not download an entire issue of a journal or multiple copies of articles, and you may use content in the JSTOR archive only for your personal, non-commercial use.

Each copy of any part of a JSTOR transmission must contain the same copyright notice that appears on the screen or printed page of such transmission.

Science is published by American Association for the Advancement of Science. Please contact the publisher for further permissions regarding the use of this work. Publisher contact information may be obtained at <http://www.jstor.org/journals/aaas.html>.

Science

©1976 American Association for the Advancement of Science

JSTOR and the JSTOR logo are trademarks of JSTOR, and are Registered in the U.S. Patent and Trademark Office. For more information on JSTOR contact jstor-info@umich.edu.

©2003 JSTOR

the enhancement of ^{129}Xe . A determination of the relative abundances of the other isotopes requires additional analyses of enriched samples. It is generally agreed that ^{129}Xe anomalies in meteoritic and terrestrial gas samples result from the production of this isotope by decay of extinct ^{129}I (12). We find that the ratio of ^{129}Xe to ^{132}Xe is 2.5 (+ 2 or - 1); the terrestrial atmospheric value is 0.97, and in the carbonaceous and ordinary chondrites, values as high as 4.5 and 9.6 have been reported (6, 7, 12). There is a tendency for more ^{129}Xe in meteorites of types C-3 and C-4 than types C-1 or C-2, which may be attributable to the greater ability of the coarse-grained C-3 and C-4 types to retain the ^{129}Xe than the fine-grained C-1 and C-2 types, according to Mazor *et al.* (7). One might therefore conjecture that a planetary atmosphere derived from a partially degassed veneer enriched in material of type C-1 would show an enhancement of ^{129}Xe ; but one might also expect such an enhancement in an atmosphere that had suffered massive losses at an appropriate interval after formation of the planet.

These are only two of several hypotheses that could explain the observations, however, and we shall study these problems in more detail after we have obtained results from the experiments planned for the end of the extended mission.

T. OWEN

Department of Earth and Space Sciences, State University of New York, Stony Brook 11794

K. BIEMANN

Department of Chemistry, Massachusetts Institute of Technology, Cambridge 02139

D. R. RUSHNECK

Interface, Inc., Post Office Box 297, Fort Collins, Colorado 80522

J. E. BILLER

Department of Chemistry, Massachusetts Institute of Technology

D. W. HOWARTH

Guidance and Control Systems Division, Litton Industries, Woodland Hills, California 91364

A. L. LAFLEUR

Department of Chemistry, Massachusetts Institute of Technology

References and Notes

1. T. Owen and K. Biemann, *Science* **193**, 801 (1976). K. Biemann, T. Owen, D. R. Rushneck, A. L. LaFleur, D. W. Howarth, *ibid.* **194**, 76 (1976).
2. K. Biemann, J. Oro, P. Toulmin III, L. E. Orgel, A. O. Nier, D. M. Anderson, P. G. Simmonds, D. Flory, A. V. Diaz, D. R. Rushneck, J. E. Biller, *ibid.* **194**, 72 (1976).
3. T. Owen, *Comments Astrophys. Space Phys.* **5**, 175 (1974).
4. C. A. Barth, *Annu. Rev. Earth Planet. Sci.* **2**, 33 (1974).
5. One could argue that the noble gases were originally present on Mars in a "cosmic" ratio, in

- which case the $^{36}\text{Ar}/\text{Kr}$ ratio would be 2.5×10^3 and $\text{Kr}/\text{Xe} \approx 9$ [A. G. W. Cameron, *Space Sci. Rev.* **15**, 121 (1973)]. The Ar/Kr ratio would then have been reduced to its present earthlike value coincidentally by solar wind sweeping. This seems to ask a lot both from coincidence and from the solar wind, but a definitive test would be the detection of neon, which may yet be possible. (The enhancement of ^{129}Xe also argues against a strictly cosmic noble gas inventory.)
6. P. Signer, in *The Origin and Evolution of Atmospheres and Oceans*, P. J. Brancazio and A. G. W. Cameron, Eds. (Wiley, New York, 1964), chap. 8.
 7. E. Mazor, D. Heymann, E. Anders, *Geochim. Cosmochim. Acta* **34**, 781 (1970).
 8. J. Wasson, *Nature (London)* **223**, 163 (1969).
 9. F. Fanale, *Icarus* **15**, 279 (1971).
 10. R. A. Canals, E. C. Alexander, Jr., O. K.

Manuel, *J. Geophys. Res.* **73**, 3331 (1968); F. R. Fanale and W. A. Cannon, *Earth Planet. Sci. Lett.* **11**, 362 (1971).

11. F. P. Fanale, private communication.
12. J. H. Reynolds, *J. Geophys. Res.* **68**, 2939 (1963); R. O. Pepin, in *The Origin and Evolution of Atmospheres and Oceans*, P. J. Brancazio and A. G. W. Cameron, Eds. (Wiley, New York, 1964), chap. 9.
13. We thank A. Tomassian and W. Dencker for optimizing the mass spectrometer and atmospheric filter assembly, respectively. We are indebted to A. V. Diaz, E. M. Ruiz, and R. Williams for their assistance. This work was supported by research contracts NAS 1-10493 and NAS 1-9684 from the National Aeronautics and Space Administration.

16 November 1976

Composition and Structure of the Martian Upper Atmosphere: Analysis of Results from Viking

Abstract. Densities for carbon dioxide measured by the upper atmospheric mass spectrometers on Viking 1 and Viking 2 are analyzed to yield height profiles for the temperature of the martian atmosphere between 120 and 200 kilometers. Densities for nitrogen and argon are used to derive vertical profiles for the eddy diffusion coefficient over the same height range. The upper atmosphere of Mars is surprisingly cold with average temperatures for both Viking 1 and Viking 2 of less than 200°K, and there is significant vertical structure. Model calculations are presented and shown to be in good agreement with measured concentrations of carbon monoxide, oxygen, and nitric oxide.

This report addresses a number of topics relevant to the composition and structure of the upper atmosphere of Mars. Densities of CO_2 as measured by the upper atmospheric mass spectrometers on Viking landers VL1 and VL2 (1-3) are used to determine profiles for temperature as a function of altitude. Temperatures derived in this manner are then

used to analyze height profiles as measured for the concentrations of N_2 and Ar. This procedure gives information on the extent to which the composition of the upper atmosphere of Mars may be influenced by mass mixing, as measured here in terms of the parameter eddy diffusion (4). The general validity of the approach may be checked by applications

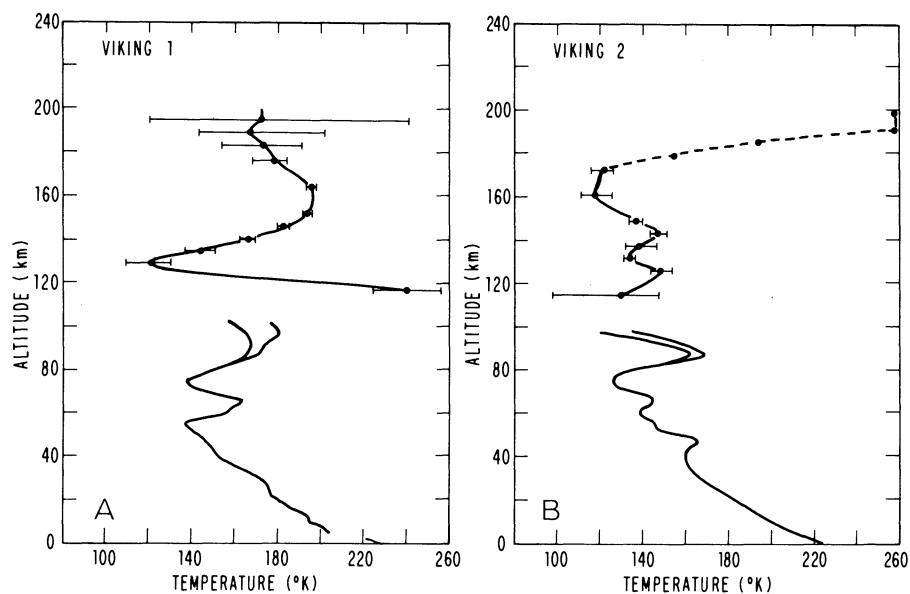


Fig. 1. (A) Temperatures for the martian atmosphere above 120 km obtained from an analysis of ion peaks at mass numbers 44, 22, and 12, as measured by VL1. Uncertainties implied by the spread in values obtained from the individual mass peaks are indicated by the error bars. Temperatures obtained by Seiff and his co-workers (1, 5) for the lower atmosphere are shown for comparison. (B) Same as (A) but for VL2. The dashed lines above 170 km indicate altitudes for which there are data only at mass number 44.

to CO and O₂. Finally, photochemical theory is used to calculate height-dependent concentrations of NO, and the results are compared with the measurements obtained by VL1.

Carbon dioxide is the major constituent of the martian atmosphere at all altitudes of the interest to the present investigation. Mass density ρ and pressure p obey the well-known barometric relation

$$\frac{dp}{dz} = -\rho g \quad (1)$$

where g defines the local acceleration of gravity. Equation 1 may be recast in the form

$$n(z_2) = \frac{T_1 n(z_1)}{T_2} \exp\left(-\int_{z_1}^{z_2} \frac{dz}{H}\right) \quad (2)$$

where $n(z_1, z_2)$ indicates the density of CO₂ at heights z_1 and z_2 , $T_{1,2}$ denotes the corresponding temperatures, and H is the scale height given by

$$H = \frac{kT}{mg} \quad (3)$$

Here k is Boltzmann's constant, and m defines the mass of CO₂. Equation 2 is essentially exact at high altitudes. It should be adjusted to reflect a smaller mean molecular weight at lower altitudes in order to take account of the influence of mass mixing. The modification at lower altitudes is trivial, however, in the present context, introducing uncertainties in temperatures obtained from Eq. 2 of no more than about 5 percent.

Equation 2 may be used in an iterative scheme to determine temperature as a function of altitude on the basis of the

Table 1. Eddy diffusion coefficients (in square centimeters per second) as derived from an analysis of height profiles for Ar and N₂.

Altitude (km)	VL1	VL2
170	1.2×10^9	4.2×10^9
160	5.9×10^8	2.0×10^9
150	2.8×10^8	9.3×10^8
140	1.3×10^8	4.4×10^8
130	6.2×10^7	2.1×10^8
120	5.0×10^7	9.8×10^7
110	5.0×10^7	4.6×10^7
100	5.0×10^7	2.1×10^7

density profiles for CO₂ presented elsewhere (3). The iteration proceeds from the top, with the atmosphere taken as isothermal over the altitude interval spanned by the first two data points. Temperatures may be derived in an independent fashion from densities found from analysis of ion peaks measured at mass numbers 44, 22, and 12. The divergence of results gives an indication of the absolute accuracy of the method. Results are shown in Fig. 1, which includes also, for purposes of comparison, temperatures derived for the lower atmosphere by Seiff and his co-workers (1, 5).

The temperature profiles for both VL1 and VL2 show considerable wavelike structure at all altitudes above about 30 km. The amplitude of the wave appears to grow with altitude for VL1 over the height range 50 to 120 km, although the temperature obtained at 118 km may be rather more uncertain than the spread of values indicated by the horizontal error bars in Fig. 1A, as a result of possible pressure saturation of the upper atmospheric mass spectrometer. Temperature

lapse rates approach the adiabatic limit over several altitude intervals in both VL1 and VL2. The wave structure in VL1 may reflect the influence of the diurnal tide generated by thermal forcing of the atmosphere in the near-surface environment (6). One might interpret the structure near 100 km on VL1 as an indication that the wave has grown to a limiting amplitude, such that dissipation must exercise a major influence on further upward propagation of the diurnal tide. This conjecture is consistent with the apparent increase in vertical wavelength implied by the structure at higher altitudes. The amplitude of the wave oscillations on VL2 appears to be less than that for VL1, possibly a consequence of the higher latitude for VL2, where rotational effects might be expected to inhibit propagation of the diurnal tide.

The temperatures, as indicated by Fig. 1, are significantly less than thermospheric temperatures obtained from analyses of the airglow data on Mariner 6, Mariner 7, and Mariner 9 (7). The Viking spacecraft landed on Mars when the planet was close to aphelion, at a solar distance near 1.64 astronomical units (A.U.). In contrast, Mariner 6 and Mariner 7 encountered the planet near perihelion, at a solar distance of about 1.43 A.U. The early orbits for Mariner 9 also coincided with near-perihelion conditions. Accordingly, much of earlier deep space data for Mars may be biased toward conditions favoring a warmer thermosphere, maintained either by a higher flux of tidal energy from the lower atmosphere or by an enhanced rate for local heating due to absorption of solar ultraviolet radiation. Scale heights for the martian ionosphere as measured by Mariner 9 (8) appear to exhibit a larger scatter of values during later phases of the mission when the insolation condition may be more directly comparable to that for Viking. The topside scale height has an average value of about 38 km over the first 70 orbits for Mariner 9. Scale heights as low as 25 km were detected during orbits subsequent to rev 350.

There is an apparent indication of a rise in temperature above 170 km, as shown by the dashed curve in Fig. 1B. The data above 170 km are based exclusively on an analysis of the peak at mass 44. It is difficult, therefore, to assess the accuracy of the temperatures shown here. A change in temperature with altitude above 170 km is unexpected. The density of CO₂ at this altitude is only $6 \times 10^7 \text{ cm}^{-3}$, which would imply a mean free path of about 50 km. If we allow for the presence of atomic oxygen, using densities derived below, the mean free

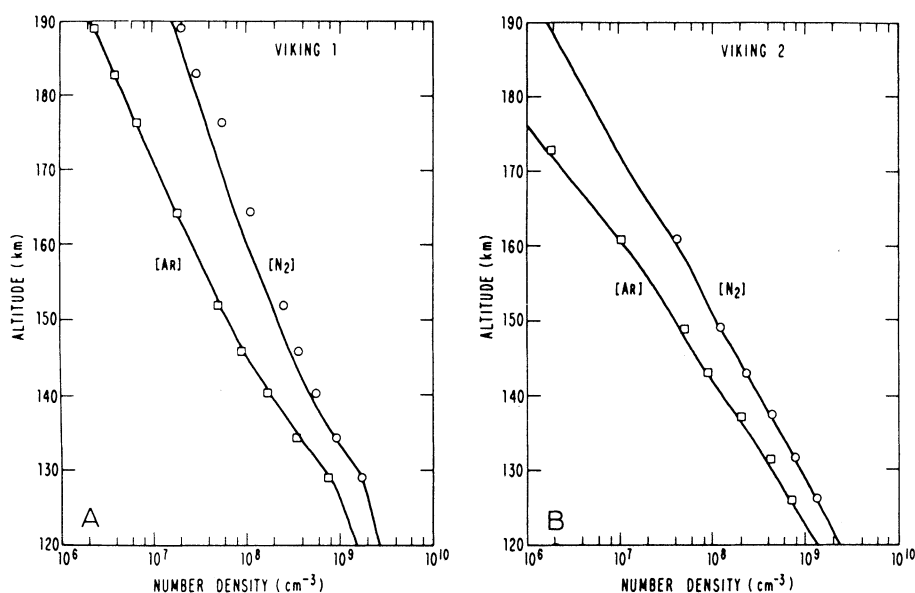


Fig. 2. (A) Upper atmospheric densities for N₂ and Ar as calculated for VL1, on the basis of eddy diffusion coefficients tabulated in Table 1. Volume mixing ratios for N₂ and Ar near the martian surface are taken as 2.4×10^{-2} and 1.5×10^{-2} . Data obtained by VL1 are indicated by \circ (N₂) and \square (Ar). (B) Same as (A) except for VL2.

path could be reduced to about 30 km. If we assume that densities at 170 km are high enough so that the energy flux may be computed directly on the basis of known values for the thermal conductivity, we may infer an energy flux of magnitude 5×10^{-2} erg cm⁻² sec⁻¹ directed downward at 170 km. This flux is too high to be explained in terms of in situ absorption of solar ultraviolet radiation. It could arise, however, as a result of the transfer of energy from the post-shock solar wind. One would expect the density of CO₂ in the martian exosphere to exhibit a complex structure with altitude in this case. Regrettably, the data are not sufficiently precise to permit a more quantitative assessment of this possibility. The high-altitude thermal structure suggested by Fig. 1B is intriguing, but further work is clearly required to enhance the confidence level of the low-pressure calibration procedures employed to derive CO₂ densities at higher altitudes.

Densities for Ar and N₂ may be computed from Eq. 2, with suitable redefinition of H . The scale height in this case is given by

$$\frac{1}{H} = \frac{1}{K + D_i} \left(\frac{K}{H_{av}} + \frac{D_i}{H_i} \right) \quad (4)$$

where K denotes the magnitude of the eddy diffusion coefficient, D_i is the appropriate value for the molecular diffusion coefficient ($i = \text{Ar}$ or N_2), H_i is the scale height for the i th component ($H_i = kT/m_i g$), and H_{av} is an average scale height for the atmosphere given by $kT/m_{av} g$, where m_{av} denotes the mean molecular mass. Observed densities for Ar and N₂ may be used to deduce values for K . The results are summarized in Table 1. The quality of the fit to Ar and N₂ is illustrated in Fig. 2.

Measured concentrations for CO provide an important check on values for K derived above. We obtained concentrations for CO, O, and O₂, following procedures described by Kong and McElroy (9). Mixing ratios for CO and O₂ in the lower atmosphere were set equal to 8×10^{-4} and 1.6×10^{-3} , respectively, consistent with ground-based spectroscopic data (10). The agreement of the model with measured profiles for CO and O₂ is satisfactory, as indicated by Fig. 3, lending confidence to the procedures adopted earlier to derive values for K and T .

A model for the martian ionosphere appropriate for VL1 is shown in Fig. 4A. Details of the model are summarized in Table 2. The ratio O₂⁺/CO₂⁺ appears to be somewhat less than values obtained from the retarding potential analyzer on VL1 (1). The discrepancy may indicate the need for a somewhat larger concen-

Table 2. Important ionospheric reactions in the martian ionosphere. Photodissociation rates at the top of the atmosphere are given in reciprocal seconds. Two-body reaction rates (k) are cubic centimeters per second.

Reaction	Rate coefficient	Referen
CO ₂ + $h\nu$ → CO ₂ ⁺ + e	$J_1 = 2.4 \times 10^{-7}$	(14)
N ₂ + $h\nu$ → N ₂ ⁺ + e	$J_2 = 8.7 \times 10^{-8}$	(14)
O + $h\nu$ → O ⁺ + e	$J_3 = 2.7 \times 10^{-7}$	(14)
CO + $h\nu$ → CO ⁺ + e	$J_4 = 4.4 \times 10^{-7}$	(14)
CO ₂ ⁺ + O → CO + O ₂ ⁺	$k_1 = 1.6 \times 10^{-10}$	(15)
CO ₂ ⁺ + O → CO ₂ + O ⁺	$k_2 = 1.0 \times 10^{-10}$	(15)
N ₂ ⁺ + CO ₂ → N ₂ + CO ₂ ⁺	$k_3 = 9 \times 10^{-10}$	(15)
O ⁺ + CO ₂ → CO + O ₂ ⁺	$k_5 = 1 \times 10^{-9}$	(16)
CO ⁺ + CO ₂ → CO + CO ₂ ⁺	$k_6 = 1 \times 10^{-9}$	(16)
CO ₂ ⁺ + NO → CO ₂ + NO ⁺	$k_7 = 1.2 \times 10^{-10}$	(15)
O ₂ ⁺ + NO → O ₂ + NO ⁺	$k_8 = 6.3 \times 10^{-10}$	(17)
CO ₂ ⁺ + e → CO + O	$k_9 = 3.8 \times 10^{-7}$	(18)
O ₂ ⁺ + e → O + O	$k_{10} = 2.2 \times 10^{-7} \left(\frac{300}{T} \right)$	(18)
NO ⁺ + e → N + O	$k_{11} = 4.3 \times 10^{-7} \left(\frac{300}{T} \right)^{0.37}$	(19)

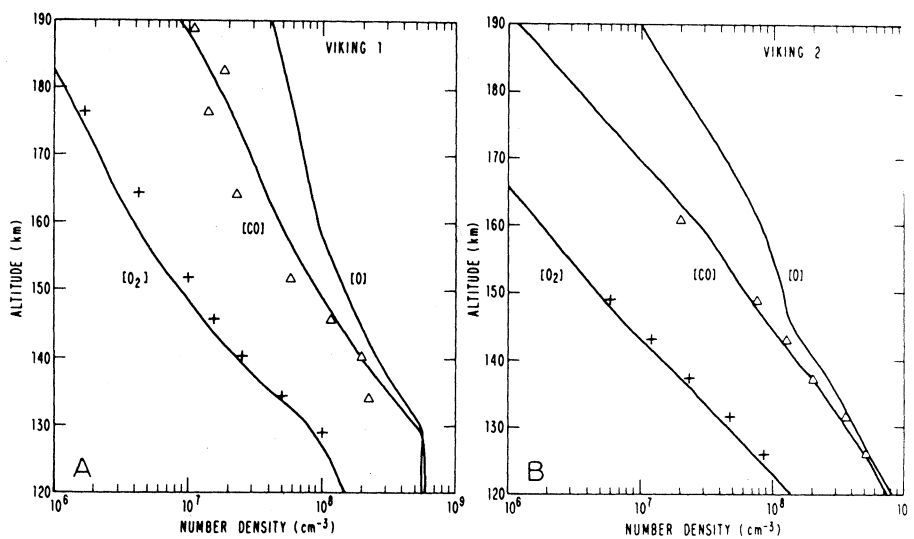


Fig. 3. (A) Upper atmospheric densities for CO, O₂, and O calculated for VL1, based on eddy diffusion coefficients tabulated in Table 1. Volume mixing ratios for CO and O₂ near the martian surface are taken as 8×10^{-4} and 1.6×10^{-3} , respectively. Data obtained by VL1 are indicated by Δ (CO) and + (O₂). (B) Same as (A) except for VL2.

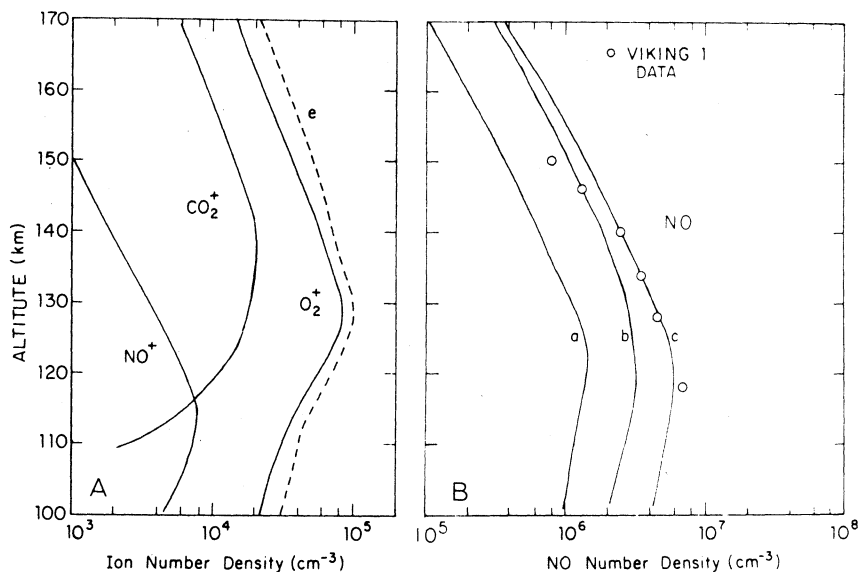


Fig. 4. (A) Number densities for the martian ionosphere computed with rate constants given in Table 2. Minor ions with densities less than 10^3 cm⁻³ are omitted. (B) Comparison of computed and measured number densities of NO in the upper atmosphere of Mars. Computational methods are described in (12).

tration of O than values indicated in Fig. 3. Alternatively, the discrepancy could be removed if small adjustments were made in the rate constants for the reactions



and

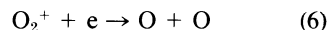


Figure 4B shows a comparison of observed and computed values for the concentration of NO. We obtained curve a by using cross sections for the electron impact dissociation of N₂ as measured by Winters (11) with a quantum yield for N(²D) taken equal to 50 percent (12). Curve b allowed for an increase in the cross sections for e + N₂ by a factor of 5 for all energies below 40 ev, an adjustment suggested by recent laboratory measurements by Zipf (13). The quantum yield for N(²D) was set equal to 50 percent in curve b. It was increased to 75 percent in curve c, for which the cross section for e + N₂ was taken equal to three times the value given by Winters (11) at impact energies below 40 ev. Model calculations are in satisfactory accord with observational data. It would appear that the remaining uncertainties may be removed as a result of suitable laboratory experimentation.

The analysis given here implies mixing ratios for N₂, Ar, and O₂ in the bulk atmosphere of magnitude 2.4×10^{-2} , 1.5×10^{-2} , and 1.6×10^{-3} , respectively. The upper atmosphere is enriched in CO and NO relative to the composition of the lower atmosphere, for which we derive mixing ratios of 8×10^{-4} and between 10^{-8} and 10^{-9} , respectively.

M. B. MCELROY

T. Y. KONG

Y. L. YUNG

Center for Earth and Planetary
Physics, Harvard University,
Cambridge, Massachusetts 02138

A. O. NIER

School of Physics and Astronomy,
University of Minnesota,
Minneapolis 55455

References and Notes

1. A. O. Nier, W. B. Hanson, A. Seiff, M. B. McElroy, N. W. Spencer, R. J. Duckett, T. C. D. Knight, W. S. Cook, *Science* **193**, 786 (1976).
2. A. O. Nier, M. B. McElroy, Y. L. Yung, *ibid.* **194**, 68 (1976).
3. A. O. Nier and M. B. McElroy, *ibid.*, p. 1298.
4. H. Lettau, in *Compendium of Meteorology*, T. F. Malone, Ed. (American Meteorological Society, Boston, 1951), pp. 320-333.
5. A. Seiff and D. B. Kirk, *Science* **194**, 1300 (1976).
6. R. W. Zurek, *J. Atmos. Sci.* **33**, 321 (1976).
7. C. A. Barth, A. I. Stewart, C. W. Hord, A. L. Lane, *Icarus* **17**, 457 (1972).
8. A. J. Kliore, G. Fjeldbo, B. L. Seidel, M. J. Sykes, P. M. Woiceshyn, *J. Geophys. Res.* **78**, 4331 (1973).
9. T. Y. Kong and M. B. McElroy, *Icarus*, in press.
10. L. D. Kaplan, J. Connes, P. Connes [*Astrophys.*

J. **157**, L187 (1969)] gave a CO/CO₂ mixing ratio of 8×10^{-4} . N. P. Carleton and W. A. Traub [*Science* **177**, 988 (1972)] obtained an O₂/CO₂ mixing ratio of $1.3 (\pm 0.3) \times 10^{-3}$. Both values are consistent with numbers used in the present calculation.

11. H. F. Winters, *J. Chem. Phys.* **44**, 1472 (1966).
12. Y. L. Yung, D. F. Strobel, T. Y. Kong, M. B. McElroy, *Icarus*, in press.
13. E. Zipf, personal communication.
14. Calculated on the basis of solar and cross-section flux as tabulated in (15).
15. M. H. Bortner and T. Bauer, Eds., *Reaction Rate Handbook* (General Electric, Tempo, Santa Barbara, Calif., 1972).

16. F. C. Fehsenfeld, A. L. Schmeltekopf, D. B. Dunkin, E. E. Ferguson, *Environ. Sci. Serv. Admin. Tech Rep. ERL 135* (1969), p. AL3.
17. F. C. Fehsenfeld, D. B. Dunkin, E. E. Ferguson, *Planet. Space Sci.* **18**, 1267 (1970).
18. J. N. Bardsley and M. A. Biondi, *Adv. Ar. Mol. Phys.* **6**, 1 (1970).
19. C. M. Huang, M. A. Biondi, R. Johnsen, *Phys. Rev. A* **11**, 901 (1975).
20. Work at the University of Minnesota and at Harvard University was supported under NASA contracts NAS-1-9697 and NAS-1-10492, respectively.

12 November 1976

Structure of the Neutral Upper Atmosphere of Mars:

Results from Viking 1 and Viking 2

Abstract. *Neutral mass spectrometers carried on the aeroshells of Viking 1 and Viking 2 indicate that carbon dioxide is the major constituent of the martian atmosphere over the height range 120 to 200 kilometers. The atmosphere contains detectable concentrations of nitrogen, argon, carbon monoxide, molecular oxygen, atomic oxygen, and nitric oxide. The upper atmosphere exhibits a complex and variable thermal structure and is well mixed to heights in excess of 120 kilometers.*

The scientific payload of the Viking landers VL1 and VL2, which landed on Mars on 20 July 1976 and 3 September 1976, respectively, included mass spectrometers designed to measure properties of the neutral atmosphere over the approximate height range 120 to 200 km. The upper atmosphere of Mars consists mainly of CO₂, with trace-detectable quantities of N₂, Ar, CO, O₂, O, and NO (1, 2). The isotopic composition of carbon and oxygen in the martian atmosphere is similar to that observed for the terrestrial atmosphere. The martian atmosphere is enriched, however, in ¹⁵N relative to ¹⁴N (2, 3). The ratio ¹⁵N/¹⁴N for Mars exceeds the value for Earth by a factor of about 1.75, a result which may be taken to indicate a denser nitrogen atmosphere for Mars in the past (2, 4). The enrichment of ¹⁵N is thought to be due to past selective escape of ¹⁴N (2, 4, 5).

This report gives an updated account of results obtained by VL1, together with a preliminary report on data from VL2. We emphasize results relevant to the question of atmospheric structure. An analysis of the manner in which the density of CO₂ varies as a function of altitude may be used to obtain information on the thermal structure of the upper atmosphere of Mars. The variation in the densities of other gases, N₂ and Ar in particular, with altitude may be used to study the extent to which the upper atmosphere is influenced by mass mixing processes, associated perhaps with the dissipation of inertial gravity waves. The upper atmosphere of Mars is surprisingly cold and variable. Mass mixing is more efficient for Mars than for Earth. If we use as a measure of the mixing process

an effective eddy diffusion coefficient, it is clear that this parameter must have values in the range 10^8 to 10^9 cm² sec⁻¹ over the altitude interval 120 to 150 km on Mars, which may be compared to a value of order 10^6 cm² sec⁻¹ thought to apply at similar altitudes in Earth's atmosphere (6).

The data discussed here were obtained with instruments mounted on the spacecraft aeroshell, with open ion sources which allowed gas to freely enter the ionizing region of the spectrometers (7). The sensitivity of the instruments was enhanced by the ram effect produced as a result of the high speed of the spacecraft, about 4.5 km sec⁻¹. Complications introduced by the ram effect are well understood, and the raw data may be reliably interpreted to yield ambient densities, on the basis of reduction techniques discussed elsewhere (8).

The experiment has a number of redundant features which may be exploited in order to enhance confidence in the interpretation of the measurements. There are a variety of mass peaks which may be used to obtain information on the density of individual species. For example, ionization of argon by 75-ev electrons, one of two energy options used on Viking, leads to peaks at mass numbers 40 and 20, associated with the formation of Ar⁺ and Ar²⁺. The relative magnitude of these peaks, about 5 to 1, is known on the basis of preflight calibration of the instruments. Ionization of CO₂ gives peaks at mass numbers 44, 28, 22, 16, and 12 associated with CO₂⁺, CO⁺, CO₂²⁺, O⁺, and C⁺. The presence of CO may be inferred from peaks at mass numbers 28, 16, 14, and 12. Because CO is a minor